European Review for Medical and Pharmacological Sciences 2020; 24: 3049-3061

The long non-coding RNA DDX11-AS1 facilitates cell progression and oxaliplatin resistance *via* regulating miR-326/IRS1 axis in gastric cancer

W. SONG[1], Y. QIAN[2], M.-H. ZHANG[1], H. WANG[1], X. WEN[1], X.-Z. YANG[1], W.-J. DAI[1]

[1]Department of Gastroenterology, The Affiliated Huai'an No. 1 People's Hospital of Nanjing Medical University, Huai'an, China
[2]Department of General Surgery, The Affiliated Huai'an No. 1 People's Hospital of Nanjing Medical University, Huai'an, China

Abstract. – OBJECTIVE: The long non-coding RNA DDX11 antisense RNA 1 (DDX11-AS1) was found to be highly expressed in gastric cancer (GC). This study was to explore the role and molecular mechanism in oxaliplatin (OXA) resistance.

PATIENTS AND METHODS: The levels of DDX11-AS1, microRNA-326 (miR-326) and insulin receptor substrate 1 (IRS1) were measured by quantitative Real-time polymerase chain reaction (qRT-PCR). Cell proliferation, migration, invasion and apoptosis were examined by methylthiazolyldiphenyl-tetrazolium bromide (MTT), transwell and flow cytometry assays, respectively. Levels of all protein were detected using Western blot. The correlation between miR-326 and DDX11-AS1/IRS1 was confirmed by Dual-Luciferase reporter and RNA immunoprecipitation (RIP) assays. The xenograft model was constructed to explore the effect of DDX11-AS1 *in vivo*.

***RESULTS:* DDX11-AS1 was overexpressed in OXA-resistant GC tissues and cells, and DDX11-AS1 knockdown inhibited cell proliferation, migration, invasion and OXA resistance, and promoted apoptosis in OXA-resistant GC cells. Mechanically, DDX11-AS1 directly targeted miR-326 and miR-326 could bind to IRS1 in OXA-resistant GC cells. Functionally, silencing DDX11-AS1 repressed the progression and OXA resistance in OXA-resistant GC cells by down-modulating IRS1 expression via sponging miR-326 *in vitro* and *in vivo*.**

CONCLUSIONS: DDX11-AS1 accelerated the progression and OXA chemoresistance of GC cells *in vitro* and *in vivo* by sponging miR-326, thus increasing the expression of IRS1, suggesting DDX11-AS1 might be a promising prognostic biomarker and therapeutic target in GC.

Key Words:
Gastric cancer, Oxaliplatin resistance, DDX11-AS1, MiR-326, IRS1.

Introduction

Gastric cancer (GC) is a malignant gastrointestinal tumor, which has the second highest incidence and mortality rate in human cancers in China[1]. Although the clinical treatment of GC has improved, the 5-year survival rate is still low[2]. In recent years, oxaliplatin (OXA), a third-generation platinum compound, is increasingly being used to treat patients with advanced GC, but the drug resistance becomes a great challenge. Meanwhile, the pathogenesis of GC is still ambiguous, so it is of great significance to explore the molecular mechanism of tumorigenesis and OXA resistance in GC.

With the development of sequencing technology, long non-coding RNAs (lncRNAs) have come into our sight[3]. Accumulated evidence suggested that lncRNA could involve in the regulation of tumor development and chemoresistance in GC. Interstingly, interfering lncRNA HULC in GC cells induced cisplatin-stimulated cell apoptosis[4]. LncRNA CASC2 knockdown elevated cell cisplatin resistance in GC by targeting miR-19a[5]. In addition, Wu et al[6] found that lncRNA BLACAT1 facilitated OXA resistance of GC by modulating miR-361/ABCB1 axis.

DDX11 antisense RNA 1 (DDX11-AS1) was demonstrated to be an oncogene in hepatocellular carcinoma[7,8] and colorectal cancer[9]. It could regulate the tumor progression by influencing the biological behavior of cells. Furthermore, Liu et al[10] revealed that DDX11-AS1 was up-regulated in GC tissues, suggesting DDX11-AS1 might have carcinogenic functions, but the specific molecular mechanism and its role in GC chemoresistance remain unknown.

Corresponding Author: Weijie Dai, MD; e-mail: rhxbod@163.com

MicroRNAs (miRNAs) are also one of the ncRNAs that have been widely recognized to play a pivotal role in tumor growth and metastasis[11]. MiR-326 was reported to be reduced by acting as a tumor suppressor in many cancers, including breast cancer[12], cervical cancer[13] and prostatic carcinoma[14]. In GC, miR-326 was also found to down-modulate and hinder cell growth[15]. Importantly, miR-326 expression was related to the survival of colorectal cancer patients treated with OXA[16]. However, the effect of miR-326 in OXA resistance of GC is not studied yet.

As a signal docking protein, insulin receptor substrate 1 (IRS1) is able to integrate different signals and deliver them to intracellular pathways[17]. Baserga[18] supported that IRS1 acted as an oncogene to promote cell growth, metastasis and differentiation. Besides, miR-1271 could target IRS1 to regulate cisplatin resistance in GC cells[19]. However, the mechanism of IRS1 in GC and whether it could regulate OXA resistance remain to be explored. In this paper, the purpose was to investigate the role of DDX11-AS1 on the progression of OXA-resistant GC and to explore the potential molecular mechanism of DDX11-AS1.

Patients and Methods

Tissue Samples and Cell Culture

Between February 2017 and January 2019, the tumor tissues and adjacent normal tissues from 58 GC patients were obtained at The Affiliated Huai'an No.1 People's Hospital of Nanjing Medical University. These GC patients had written informed consents and had not received any treatment before the tissues were collected. The tumor tissues were divided into two groups according to their sensitivity to OXA: resistant (n=29) and sensitive (n=29). Besides, our study was permitted by the Human Ethics Committee of the Affiliated Huai'an No.1 People's Hospital of Nanjing Medical University.

GC cell lines MKN45 and AGS were obtained from Procell (Wuhan, China). To establish the drug-resistant GC cell line, MKN45 and AGS cells were exposed to sequentially increasing concentration (7.5 μM) of OXA. Finally, the OXA concentration was increased to 240 μM, and the cells were continuously maintained in 240 μM OXA. These cells were maintained in Roswell Park Memorial Institute-1640 (RPMI-1640, Thermo Fisher Scientific, Waltham, MA, USA) with 10% fetal bovine serum (FBS, Thermo Fisher Scientific) at 37°C with 5% CO_2.

Quantitative Real-Time Polymerase Chain Reaction (qRT-PCR)

GC tissues and transfected cells were collected for the extraction of total RNA using TRIzol reagent (Thermo Fisher Scientific). Then, complementary DNA (cDNA) was synthesized by a PrimeScript™ RT reagent Kit (TaKaRa, Dalian, China), and qRT-PCR was conducted on a 7500 Real-Time PCR System (Applied Biosystems, Foster City, CA, USA) using the SYBR® Premix DimerEraser Kit (TaKaRa). Glyceraldehyde-3-phosphate dehydrogenase (GAPDH) and U6 were used to act as the internal controls for lncRNA/mRNA and miRNA, respectively. Sequence of primers as follows: DDX11-AS1, Forward (F): 5'-TTAGGAGGACAACGAATCACCTC-3', Reverse (R): 5'-GTCATCTCCCAGAACCAGACTTT-3'. GAPDH, F: 5'-TGACTTCAACAGCGACACCCA-3', R: 5'-CACCCTGTTGCTGTAGCCAAA-3'. miR-326, F: 5'-CCTCTGGGCCCTTCCTCCAG-3', R: 5'-GCTGTCAACGATACGCTACCTA-3'. U6, F: 5'-CTCGCTTCGGCAGCACA-3', R: 5'-AACGCTTCACGAATTTGCGT-3'. IRS1, F: 5'-ACTGGACATCACAGCAGAATGA-3', R: 5'-AGAACGTGCAGTTCAGTCAA-3'.

Cell Proliferation Assay

MKN45 and AGS cells were tiled into the 96-well plates overnight. Cells were subsequently exposed to different doses of OXA. After 48 h, 20 μL of methylthiazolyldiphenyl-tetrazolium bromide (MTT) was added into the well for another 3 h, 100 μL dimethyl sulfoxide (DMSO, Beyotime, Beijing, China) was employed to dissolve formazan. Finally, the absorbance was checked by SpectraMax M3 microplate reader (Molecular Devices, Sunnyvale, CA, USA) at 570 nm.

Transfection

To knockdown of DDX11-AS1, small interfering RNA specifically targeting DDX11-AS1 (si-DDX11-AS1) and the control si-NC, short hairpin RNA targeting DDX11-AS1 (sh-DDX11-AS1) and the control sh-NC were synthesized by GenePharma (Shanghai, China). Hsa-miR-326 mimic (miR-326)/mimic control (miR-NC) and miR-326 inhibitor (in-miR-326)/inhibitor control (in-miR-NC) were purchased from GenePharma. For overexpression, the coding sequences (CDS) of IRS1 were inserted into the pcDNA vector (Invitrogen, Carlsbad, CA, USA). Transfections were performed in OXA-resistant GC cells using the Lipofectamine 3000 (Invitrogen, Carlsbad, CA, USA).

Transwell Assay

Both cell migration and invasion were detected by Transwell assay, the only difference was that the chambers needed to be pre-coated with Matrigel (BD Biosciences, Franklin Lakes, NJ, USA) for detection cell invasion. Briefly, MKN45/OXA and AGS/OXA cells starved for 24 h were resuspended in serum-free medium, and 200 μL of cell suspension was added to the upper chambers, while 600 μL of medium with 10% FBS was placed into the lower chambers. After incubation for 24 h, cells that migrated or invaded on the surface of inserts bottom were fixed and stained with 0.1% crystal violet (Beyotime Biotechnology, Shanghai, China) for 20 min. Then the stained cells were photographed and counted with a microscope.

Cell Apoptosis Assay

To detect cellular apoptosis, Flow cytometry assay was carried out with an Annexin V fluorescein isothiocynate (FITC)/propidium iodide (PI) Apoptosis Detection Kit (BD Biosciences). After transfected MKN45/OXA and AGS/OXA cells were incubated for 48 h, cells were harvested and stained with FITC and PI for 20 min in the absence of light. The stained cells were analyzed using a FACS Caliber flow cytometer (BD Biosciences).

Western Blot Assay

Proteins extracted from OXA-resistant GC tissues and cells were denatured for 5 minutes at 100°C. Proteins were isolated by sodium dodecyl sulfate-polyacrylamide gel electrophoresis (SDS-PAGE, Beyotime) and transfected to polyvinylidene difluoride (PVDF, Beyotime) membranes. After blocked in 5% non-fat dry milk for 2 h, the membranes were incubated with the primary antibodies overnight at 4°C, and then incubated with secondary antibodies (1:5000, Abcam, Cambridge, MA, USA) for 2 h. Finally, these bands were visualized by an ECL detection kit (Thermo Fisher Scientific, Waltham, MA, USA) and the results were analyzed using ImageJ analysis software. Primary antibodies: multi-drug resistant associate protein1 (MRP1, 1:50, Abcam), multi-drug resistance gene1 (MDR1, 1:1000, Abcam), β-actin (1:5000, Abcam) and IRS1 (1:2000, Abcam).

Dual-Luciferase Reporter Assay

The correlation between miR-326 and DDX11-AS1 or IRS1 was predicted by DIANA-LncBase v2 or Micro-T CDS. The wild sequences of DDX11-AS1 or its mutant containing miR-326 binding sites or without miR-326 binding sites were cloned into the pmirGLO vector (Promega Corporation, Madison, WI, USA) to generate DDX11-AS1 wild type (WT) and DDX11-AS1 mutant type (MUT) report plasmids. Also, the IRS1 3'UTR-WT and IRS1 3'UTR-MUT report plasmids were constructed in a similar way. Then, these reporter plasmids were co-transfected with miR-326 or miR-NC into MKN45/OXA and AGS/OXA cells for 48 h. The luciferase activity was determined using a Dual-Luciferase reporter kit (Promega Corporation).

RNA Immunoprecipitation (RIP)

MKN45/OXA and AGS/OXA cells were transfected with miR-326 or miR-NC. After 48 h, RIP assay was performed using the Magna RIP RNA-Binding Protein Immunoprecipitation Kit (Millipore, Billerica, MA, USA). In brief, cells were lysed using lysis buffer, and the cell lysate was mixed with RIP buffer containing magnetic beads conjugated with Ago2 antibody or IgG antibody overnight. Next, the beads were incubated with protease K, the RNA bound to Ago2 antibody was extracted and qRT-PCR assay was applied to measure the expression of DDX11-AS1.

Nude Mice Xenograft Models

The animal experiments were approved by the Animal Care and Use Committee of the Affiliated Huai'an No.1 People's Hospital of Nanjing Medical University. AGS/OXA cells stably transfected sh-NC or sh-DDX11-AS1 were subcutaneously injected into the 4-week-old nude mice (6 mice per group). The tumor volume was measured every 7 d. After inoculation for 28 d, all mice were euthanized and the tumor weight was weighed, and xenograft tumor tissues were stored at -80°C for further extraction of RNA and protein.

Statistical Analysis

Data were analyzed by the SPSS 19.0 (IBM Corp., Armonk, NY, USA) software and appeared as the mean ± standard deviation (SD), and repeated at least three times. The difference was assessed by Student's t-test and one-way analysis of variance (ANOVA) analysis. $p < 0.05$ was considered to be significant.

Results

DDX11-AS1 was Increased in OXA-Resistant GC Tissues and Cells

To investigate the role of DDX11-AS1, qRT-PCR was performed to detect DDX11-AS1 ex-

pression in OXA-resistant GC tissues. As shown in Figure 1A, DDX11-AS1 expression was augmented in OXA-resistant GC tissues compared to OXA-sensitive GC tissues. Meanwhile, we found that DDX11-AS1 was increased in OXA-resistant GC cell lines (MKN45/OXA and AGS/OXA) in contrast to their parental cell lines (MKN45 and AGS) (Figure 1B). The results of MTT indicated that the survival rate of MKN45/OXA and AGS/OXA cells treated with different doses of OXA was higher than their parental cells (Figure 1C-D), suggesting that we had successfully built OXA-resistant GC cell models. The data indicated that DDX11-AS1 was up-regulated in OXA-resistant GC tissues and cells.

DDX11-AS1 Knockdown Suppressed the Progression of OXA-Resistant GC Cells in Vitro

Given the high expression of DDX11-AS1 in OXA-resistant GC, we next explored its intracellular functions by interfering with DDX11-AS1. As displayed in Figure 2A, DDX11-AS1 expression was markedly declined to over 2-fold in MKN45/OXA and AGS/OXA cells by transfection of si-DDX11-AS1. The results demonstrated that the survival rate (Figure 2B-C), migration and invasion (Figure 2D-E) of MKN45/OXA and AGS/OXA cells were inhibited when DDX11-AS1 was knocked down examined by MTT and Transwell assays, respectively. As expected, interference with DDX11-AS1 in MKN45/OXA and AGS/OXA cells induced cell apoptosis by Flow cytometry (Figure 2F). Besides, we measured the expression levels of drug-resistant markers MRP1 and MDR1 [20] by Western blot. As shown in Figure 2G, DDX11-AS1 knockdown in MKN45/OXA and AGS/OXA cells hampered MRP1 and MDR1 expression levels. The above results revealed that knockdown of DDX11-AS1 repressed cell proliferation, migration, invasion and OXA resistance in OXA-resistant GC cells *in vitro*, and simultaneously promoted apoptosis.

DDX11-AS1 Acted as a Sponge of miR-326

It has been widely accepted that lncRNAs can act as competing endogenous RNAs (ceRNAs) to sponge miRNAs, and thus affecting the expression of target mRNAs[21]. Therefore, we next investigated the target miRNAs of DDX11-AS1. DIANA-LncBase v2 tool predicted that there were complementary sites between DDX11-AS1 and miR-326 (Figure 3A). Dual-Luciferase reporter assay showed that miR-326 obviously restrained the luciferase activity of MKN45/OXA and AGS/OXA cells in DDX11-AS1 WT group than that the negative control, while the luciferase activity in DDX11-AS1 MUT group remained unchanged (Figure 3B-C). Furthermore, RIP assay indicated that miR-326 increased the enrichment of DDX11-AS1 in RIP-Ago1 complex compared to RIP-IgG complex in MKN45/OXA and AGS/OXA cells (Figure 3D). Then, we found that the expression pattern of miR-326 was contrary to DDX11-AS1 in OXA-resistant GC using qRT-PCR. As shown in Figure 3E, miR-326 expression was down-modulated in OXA-resistant GC tissues, and its expression was also decreased in OXA-resistant GC cell lines (MKN45/OXA and AGS/OXA) (Figure 3F) compared to their parental cell lines (MKN45 and AGS). Additionally, DDX11-AS1 knockdown strikingly fortified miR-326 expression in MKN45/OXA and AGS/OXA cells (Figure 3G). In general, DDX11-AS1 could direct bind to miR-326 and negative modulate miR-326 expression in OXA resistant GC cells.

Si-DDX11-AS1 Suppressed Cell Progression and OXA Resistance in OXA-Resistant GC Cells by Increasing miR-326 Expression

We further explored the interaction between DDX11-AS1 and miR-326. The transfection efficiency was first measured by qRT-PCR (Figure 4A). MTT assay determined that the proliferation of MKN45 and AGS cells treated with different concentrations of OXA was retarded by si-DDX11-AS1, which was weakened by co-transfection with si-DDX11-AS1 and in-miR-326 (Figure 4B-C). The results of transwell assay showed that the inhibition of si-DDX11-AS1 on migration and invasion of MKN45/OXA and AGS/OXA cells was counteracted by inhibiting miR-326 expression (Figure 4D-E). Also, the apoptosis rate of MKN45/OXA and AGS/OXA cells was induced by si-DDX11-AS1, which was inverted by in-miR-326 (Figure 4F). The suppressive effect of silencing DDX11-AS1 on the expression levels of MRP1 and MDR1 was also overturned by miR-326 knockdown (Figure 4G). These data indicated that DDX11-AS1 modulated cell progression and OXA resistance in OXA-resistant GC cells by targeting miR-326.

DDX11-AS1 Positively Regulated IRS1 Expression by Acting as the Sponge of miR-326 in OXA-Resistant GC Cells

Micro-T CDS website was used to predict the targets of miR-326 and found that the 3'UTR of

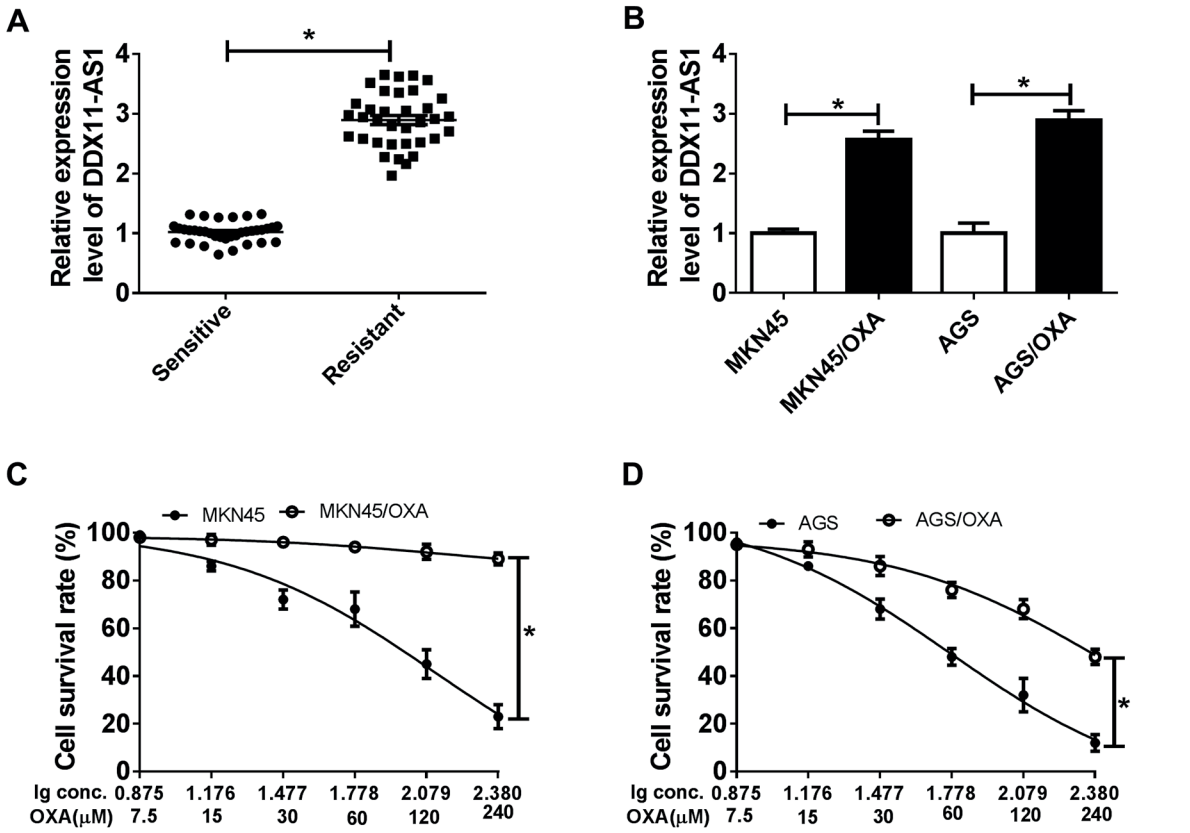

Figure 1. DDX11-AS1 was increased in OXA-resistant GC tissues and cells. **(A)** DDX11-AS1 expression in OXA-resistant GC tissues and OXA-sensitive GC tissues was detected using qRT-PCR. **(B)** DDX11-AS1 expression in OXA-resistant GC cell lines (MKN45/OXA and AGS/OXA) and their parental cell lines (MKN45 and AGS) was measured by qRT-PCR. **(C-D)** The cell proliferation was assessed using MTT assay in MKN45/OXA and AGS/OXA cells treated with different concentrations of OXA compared to their parental cells MKN45 and AGS. *$p<0.05$.

IRS1 contained the binding sites of miR-326 (Figure 5A). Similarly, Dual-Luciferase reporter assay was performed, and the results showed that miR-326 reduced the luciferase activity of MKN45/OXA and AGS/OXA cells in IRS1 3'UTR-WT group compared to the control group, there was no significant change in luciferase activity in IRS1 3'UTR-MUT group (Figure 5B-C). We also measured IRS1 expression in OXA-resistant GC tissues and cells by qRT-PCR and Western blot. As shown in Figure 5D, IRS1 mRNA expression was increased in OXA-resistant GC tissues relative to that in OXA-sensitive GC tissues, and its protein expression was also enhanced in OXA-resistant GC cell lines (Figure 5E). Besides, the effect of miR-326 on IRS1 expression was researched by Western blot. The results showed that miR-326 overexpression silenced the protein expression of IRS1, while miR-326 depletion potentiated IRS1 protein expression in MKN45/OXA and AGS/OXA cells (Figure 5F). Furthermore, DDX11-AS1 knockdown dwindled the protein expression of IRS1, and this effect could be inverted by in-miR-326 (Figure 5G). The above results revealed that DDX11-AS1 positively regulated IRS1 expression by sponging miR-326 in OXA-resistant GC cells.

Overexpression of IRS1 Reversed the Inhibitory Effect of miR-326 on Progression and OXA Resistance of OXA-Resistant GC Cells

As a target gene of miR-326, whether IRS1 could affect the function of miR-326 in OXA-resistant GC cells was unknown, so the rescue experiments were carried out. Similarly, the transfection efficiency in MKN45/OXA and AGS/OXA cells was first examined by Western blot (Figure 6A). As displayed in Figure 6B-C, after different concentrations of OXA treatment, the cell proliferation was reduced in MKN45 and AGS cells transfected with

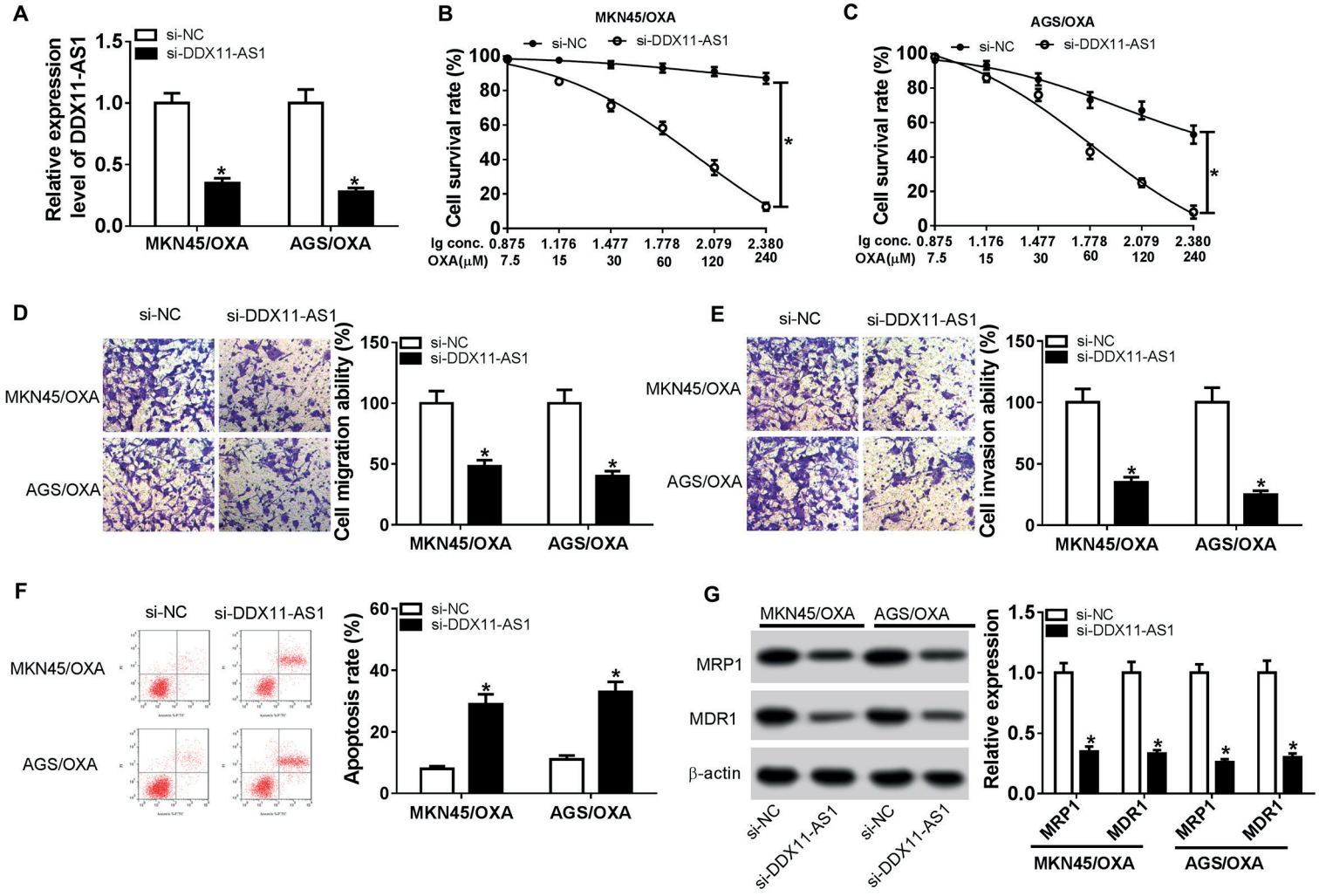

Figure 2. DDX11-AS1 knockdown suppressed the progression of OXA-resistant GC cells in vitro. **(A)** DDX11-AS1 expression in MKN45/OXA and AGS/OXA transfected with si-DDX11-AS1 or si-NC was measured using qRT-PCR. **(B-C)** The cell proliferation was examined in MKN45/OXA and AGS/OXA cells transfected with si-DDX11-AS1 or si-NC using MTT assay. **(D-E)** The migration and invasion abilities of transfected MKN45/OXA and AGS/OXA cells were determined by Transwell. (Magnification 100×). **(F)** The apoptosis of MKN45/OXA and AGS/OXA cells was detected by Flow cytometry. **(G)** The expression levels of MRP1 and MDR1 were measured by Western blot. *p<0.05.

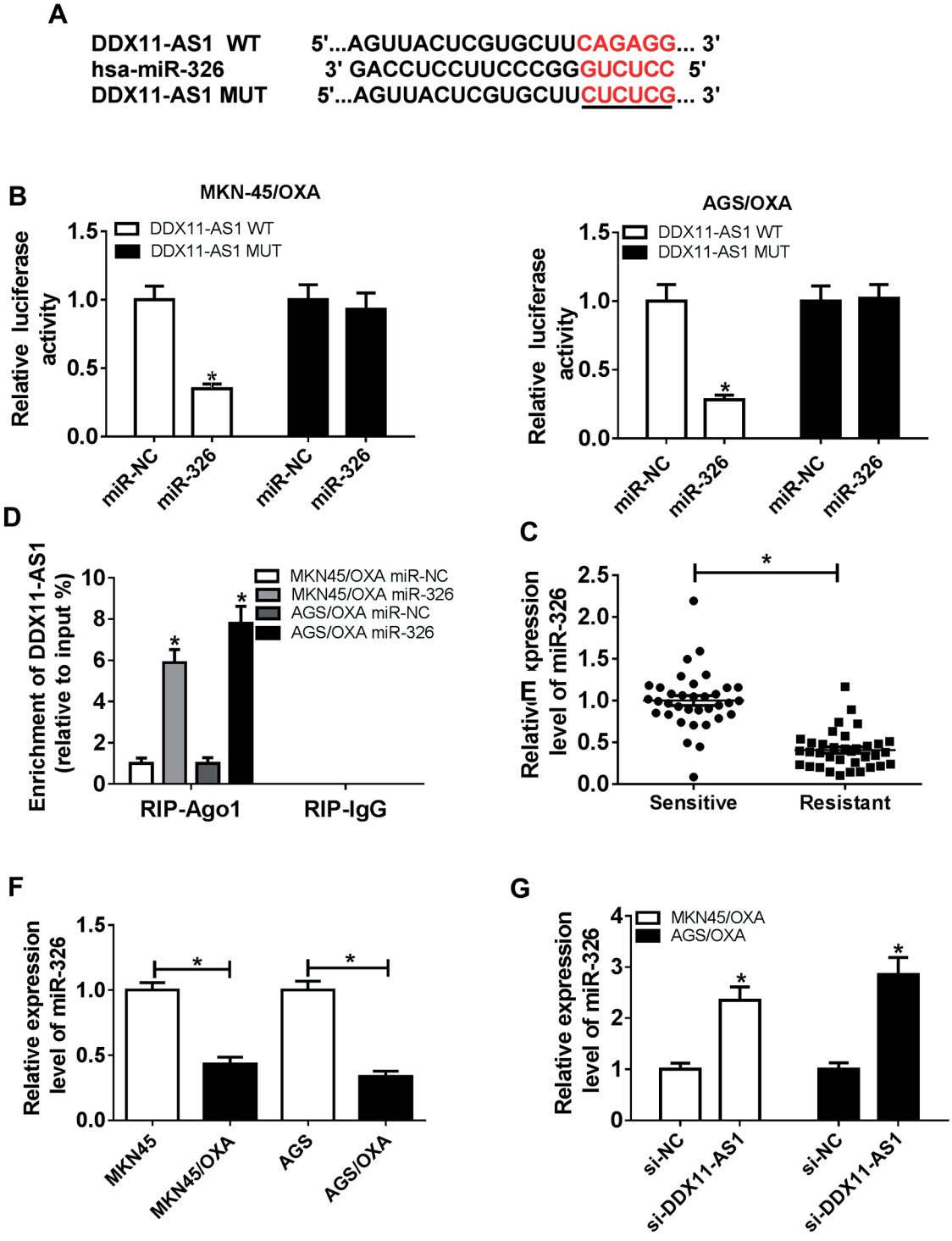

Figure 3. DDX11-AS1 acted as a sponge of miR-326. **(A)** The binding sites between DDX11-AS1 and miR-326 and the mutant sequences of DDX11-AS1 were displayed. **(B-C)** After MKN45/OXA and AGS/OXA cells were co-transfected with DDX11-AS1 WT or DDX11-AS1 MUT and miR-326 or miR-NC, the luciferase activity was analyzed by dual-luciferase reporter assay. **(D)** RIP assay was performed in MKN45/OXA and AGS/OXA cells and the enrichment of DDX11-AS1 was measured using qRT-PCR. **(E)** MiR-326 expression in OXA-resistant GC tissues and OXA-sensitive GC tissues was detected by qRT-PCR. **(F)** MiR-326 expression in OXA-resistant GC cell lines (MKN45/OXA and AGS/OXA) and their parental cell lines (MKN45 and AGS) was checked by qRT-PCR. **(G)** MiR-326 expression in MKN45/OXA and AGS/OXA cells transfected with si-DDX11-AS1 or si-NC was examined using qRT-PCR. *p<0.05.

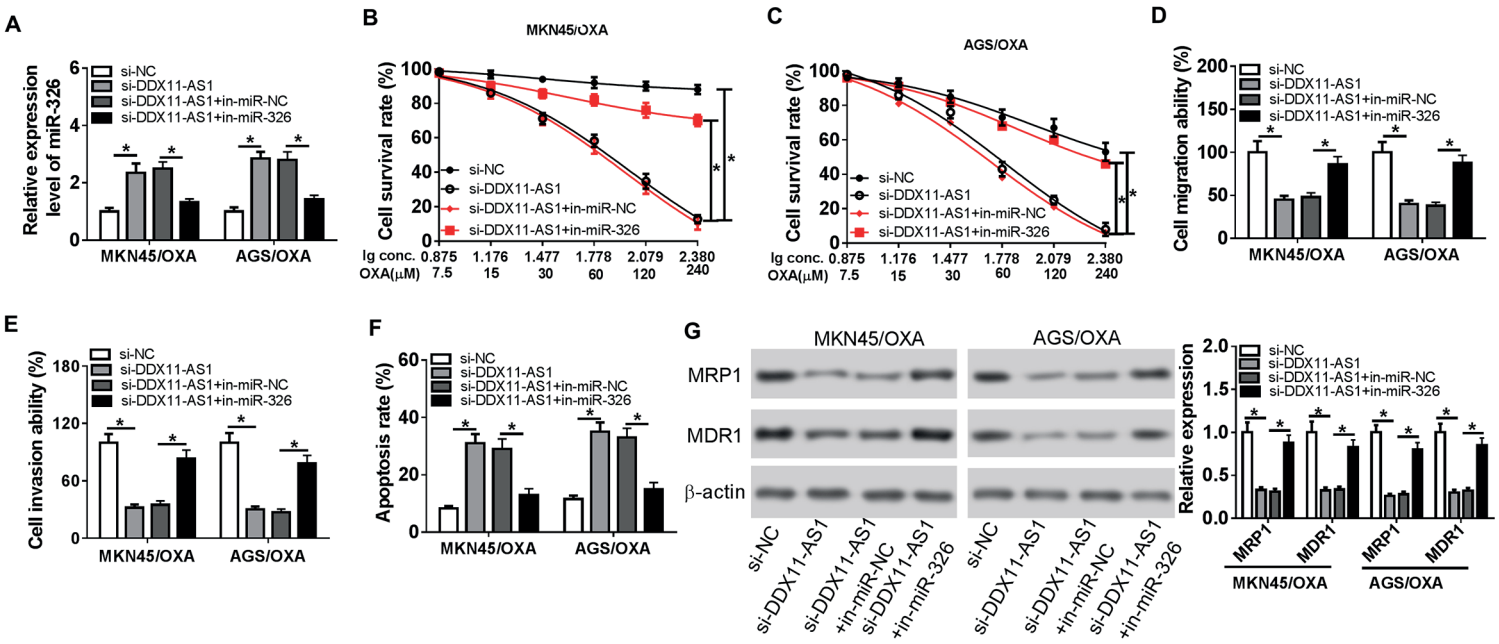

Figure 4. Si-DDX11-AS1 suppressed cell progression and OXA resistance in OXA-resistant GC cells by increasing miR-326 expression. After MKN45/OXA and AGS/OXA cells were transfected with si-NC, si-DDX11-AS1, si-DDX11-AS1 + in-miR-NC or si-DDX11-AS1 + in-miR-326. **(A)** MiR-326 expression in transfected MKN45/OXA and AGS/OXA cells was detected by qRT-PCR. **(B-C)** The proliferation of transfected MKN45/OXA and AGS/OXA cells was analyzed by MTT assay. **(D-E)** Transwell assay was used to detect cell migration and invasion. **(F)** Flow cytometry was performed to assess cell apoptosis. **(G)** The protein levels of MRP1 and MDR1 in transfected MKN45/OXA and AGS/OXA cells were measured by Western blot. *p<0.05.

miR-326, which was abrogated by overexpressing IRS1. Transwell and Flow cytometry respectively showed that up-regulation of miR-326 in MKN45/OXA and AGS/OXA cells inhibited cell migration (Figure 6D) and invasion (Figure 6E), and accelerated cell apoptosis (Figure 6F); however, these effects could be reversed by the addition of IRS1. Simultaneously, miR-326 overexpression decreased the levels of MRP1 and MDR1 in MKN45/OXA and AGS/OXA cells, and this inhibition was overturned by up-regulated IRS1 (Figure 6G). The above results revealed that miR-326 inhibited the progression and OXA resistance of OXA-resistant GC cells by targeting IRS1.

DDX11-AS1 Knockdown Suppressed the Tumor Growth in Vivo

Xenograft mice models were generated to assess the role of circ_0006528 in vivo. AGS/OXA cells transfected with sh-DDX11-AS1 or sh-NC were subcutaneously inoculated into the nude mice, and the tumor volume and weight were measured. The data revealed that silencing DDX11-AS1 drastically reduced the tumor volume (Figure 7A) and weight (Figure 7B) compared with the negative control, qRT-PCR assay showed that the expression of DDX11-AS1 was down-regulated in sh-DDX11-AS1 group (Figure 7C), while miR-326 was augmented (Figure 7D). And the protein levels of IRS1, MRP1 and MDR1 were declined in sh-DDX11-AS1 group compared to sh-NC group (Figure 7E-F). These results implied that interfering with DDX11-AS1 inhibited the tumorigenesis of OXA-resistant GC *in vivo* by regulating miR-326/IRS1 axis.

Discussion

LncRNAs could regulate the chemoresistance of multiple cancers to OXA treatment. LncRNA KCNQ1OT1 could augment the chemoresistance of OXA in colon cancer cells by regulating miR-34a/Atg4B axis[22]. And lncRNA MEG3 potentiated the sensitivity of OXA in colorectal cancer cells through targeting miR-141/PDCD4 axis[23]. In the current study DDX11-AS1 expression was enhanced in OXA-resistant GC tissues and cells. In addition, when DDX11-AS1 was knocked down in OXA-resistant GC cells, the cell proliferation, migration and invasion were inhibited, while cell apoptosis was induced. Meanwhile, the protein expression levels of drug resistance genes MRP1 and MDR1 were also decreased. These results signified that DDX11-AS1 could enhance the chemoresistance of GC cells to OXA and might be a marker of chemotherapy. Tian et al[9] showed that DDX11-AS1 served as a ceRNA of miR-873 to modulate CLDN7 expression and promoted the progression of colorectal cancer [9]. Previous reports confirmed that lncRNAs regulated the chemoresistance of OXA by acting as ceRNAs, so we speculated whether DDX11-AS1 also increased the chemoresistance of OXA in GC cells by sponging miRNAs.

Subsequently, we found that miR-326 might be a target miRNA of DDX11-AS1 through the bioinformatics website and confirmed the targeted relationship between them by Dual-Luciferase reporter and RIP assays. Although it has been previously indicated that miR-326 could serve as a tumor inhibitor to regulate the growth and metastasis of GC cells [24], whether it could regulate the chemoresistance of GC to OXA has not been studied. Our research further demonstrated that miR-326 expression was down-regulated in OXA-resistant GC tissues and cells and inversely regulated by DDX11-AS1. Moreover, the inhibition of DDX11-AS1 knockdown on progression and OXA resistance of GC cells was reversed by inhibiting miR-326 expression, suggesting silencing DDX11-AS1 suppressed the progression of OXA-resistant GC cells via targeting miR-326.

IRS1 was identified as an oncogene in human multiple cancers[25,26], including GC[27]. And IRS1 was found to be related to the chemoresistance of OXA in colon cancer cells[28]. Coincidentally, IRS1 was the target gene of miR-326 in this study, and IRS1 was highly expressed in OXA-resistant GC, which was in agreement with the data Yang et al[19]. Besides, IRS1 expression could not only be negatively regulated by miR-326, but also be positively regulated by DDX11-AS1. Functionally, miR-326 overexpression impaired the progression and chemoresistance of OXA in GC cells, while these effects were abated by overexpressing IRS1. Taken together, DDX11-AS1 facilitated the development of OXA-resistant GC cells by up-regulating IRS1 through sponging miR-326 *in vitro*. Uniformly, DDX11-AS1 promoted tumorigenesis in OXA-resistant GC by modulating miR-326/IRS1 axis.

Conclusions

In this study there have been the effects of DDX11-AS1 on proliferation, migration, invasion, apoptosis of OXA-resistant GC cells. We discovered a new DDX11-AS1/miR-326 /IRS1

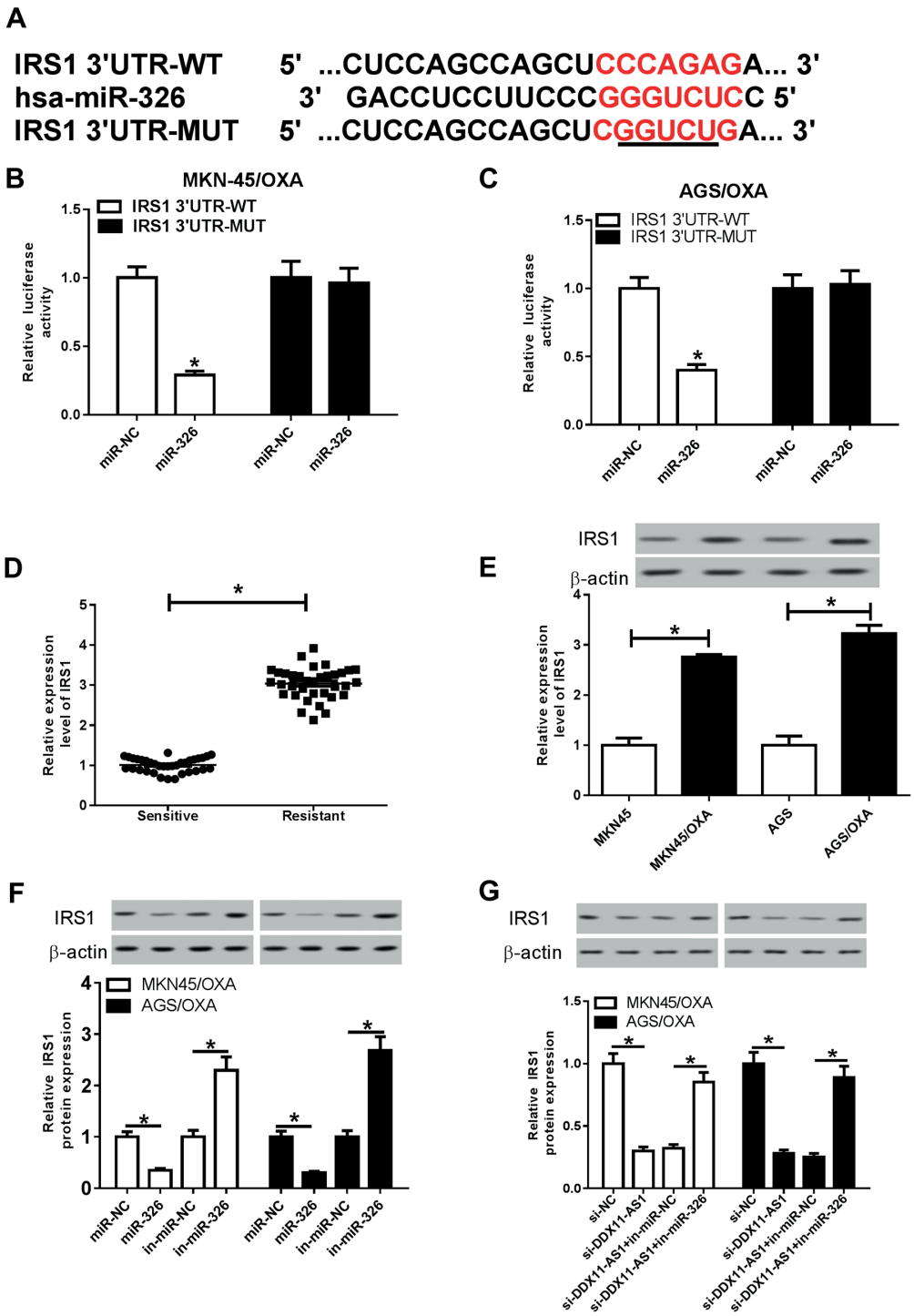

Figure 5. DDX11-AS1 positively regulated IRS1 expression by acting as the sponge of miR-326 in OXA-resistant GC cells. **(A)** The binding sites between miR-326 and IRS1 and the mutant sequences of IRS1 were showed. **(B-C)** After MKN45/OXA and AGS/OXA cells were co-transfected with IRS1 3'UTR-WT or IRS1 3'UTR-MUT and miR-326 or miR-NC, the luciferase activity was determined by dual-luciferase reporter assay. **(D)** IRS1 mRNA expression in OXA-resistant GC tissues and OXA-sensitive GC tissues was detected by qRT-PCR. **(E)** IRS1 protein expression in OXA-resistant GC cell lines (MKN45/OXA and AGS/OXA) and their parental cell lines (MKN45 and AGS) was examined by Western blot. **(F)** IRS1 protein expression in MKN45/OXA and AGS/OXA cells transfected with miR-NC, miR-326, in-miR-NC or in-miR-326 was examined using Western blot. **(G)** IRS1 protein expression in MKN45/OXA and AGS/OXA cells transfected with si-NC, si-DDX11-AS1, si-DDX11-AS1 + in-miR-NC or si-DDX11-AS1 + in-miR-326 was detected by Western blot. *p<0.05.

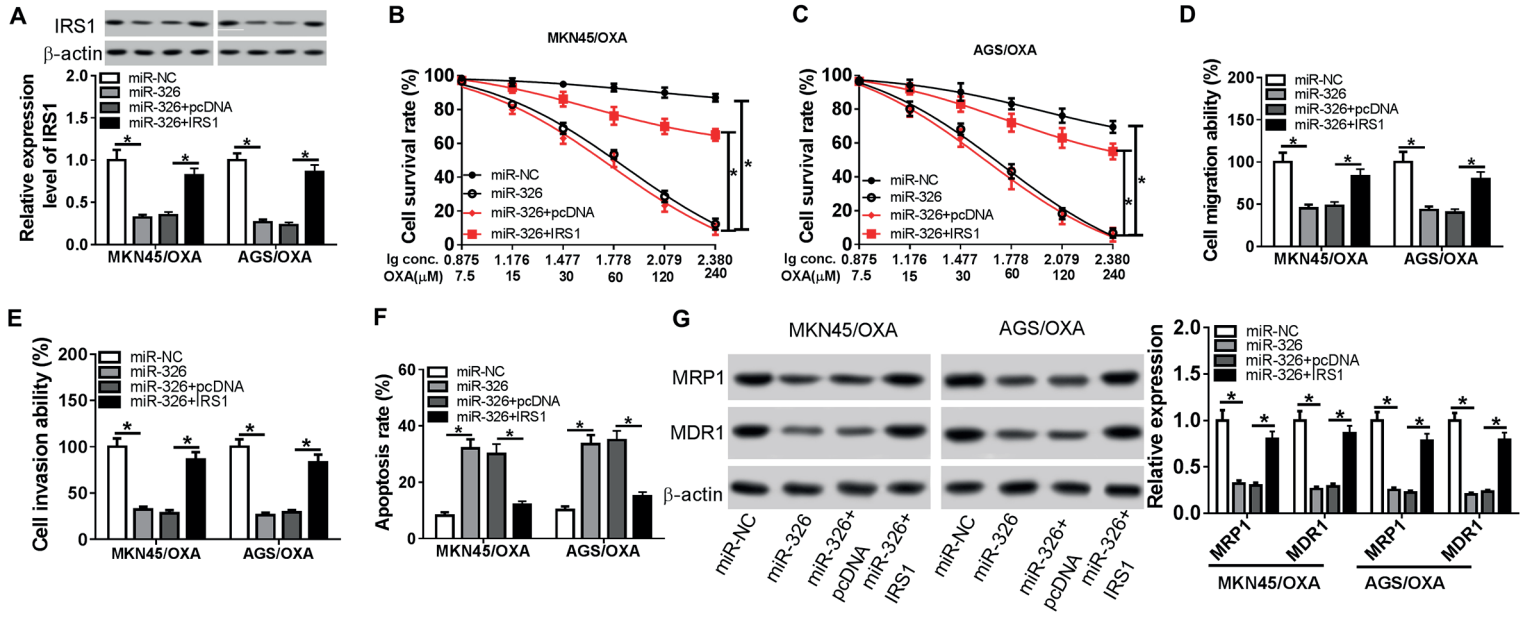

Figure 6. Overexpression of IRS1 reversed the inhibitory effect of miR-326 on progression and OXA resistance of OXA-resistant GC cells. After MKN45/OXA and AGS/OXA cells were transfected with miR-NC, miR-326, miR-326 + pcDNA or miR-326 + IRS1. **(A)** IRS1 protein expression in transfected MKN45/OXA and AGS/OXA cells was detected by Western blot. **(B-F)** The proliferation, migration, invasion and apoptosis of transfected MKN45/OXA and AGS/OXA cells were assessed by MTT, Transwell and Flow cytometry assays, respectively. **(G)** The protein levels of MRP1 and MDR1 in transfected MKN45/OXA and AGS/OXA cells were measured by Western blot. *$p<0.05$.

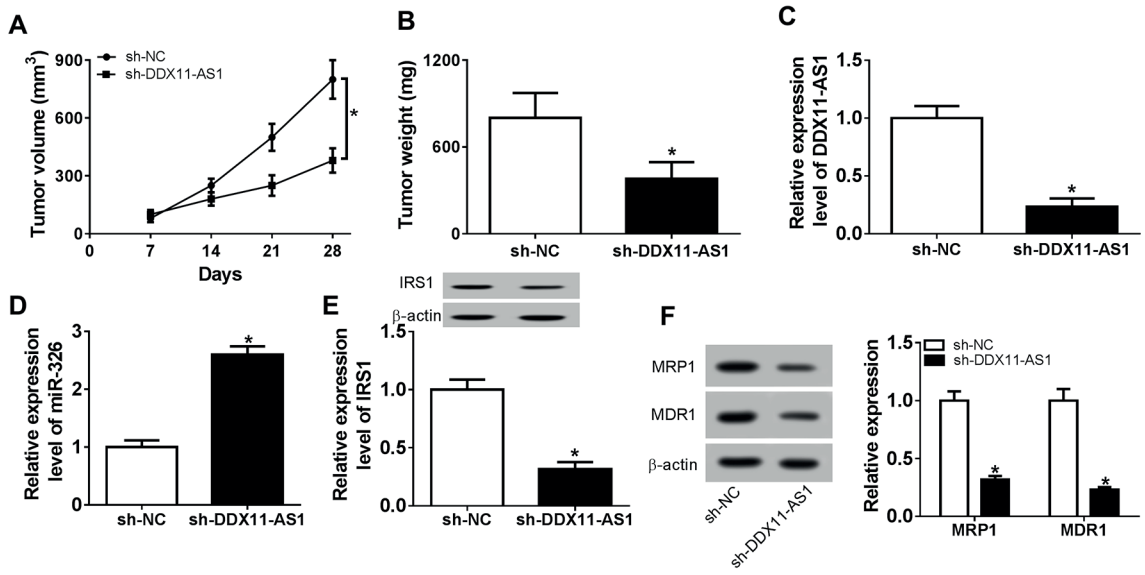

Figure 7. DDX11-AS1 knockdown suppressed the tumor growth in vivo. AGS/OXA cells were infected with sh-DDX11-AS1 or sh-NC. **(A)** Tumor volume was measured every 7 days and the tumor growth curve was depicted. **(B)** Tumor weight was detected after the mice were euthanized. **(C-D)** The levels of DDX11-AS1 and miR-326 in that tumors were examined by qRT-PCR. **(E-F)** The levels of IRS1, MRP1 and MDR1 in tumors were checked using Western blot. *$p<0.05$.

regulatory mechanism that regulated the progression of OXA-resistant GC cells *in vitro* and *in vivo*. Our study supported that DDX11-AS1 might be a potential target for the treatment of chemoresistance to OXA in patients with GC.

Conflict of Interests

The Authors declare that they have no conflict of interests.

References

1) Chen W, Zheng R, Baade PD, Zhang S, Zeng H, Bray F, Jemal A, Yu XQ, He J. Cancer statistics in China, 2015. CA Cancer J Clin 2016; 66: 115-132.
2) Fang WL, Huang KH, Chen JH, Lo SS, Hsieh MC, Shen KH, Li AF, Niu DM, Chiou SH, Wu CW. Comparison of the survival difference between AJCC 6th and 7th editions for gastric cancer patients. World J Surg 2011; 35: 2723-2729.
3) Guttman M, Rinn JL. Modular regulatory principles of large non-coding RNAs. Nature 2012; 482: 339-346.
4) Zhang Y, Song X, Wang X, Hu J, Jiang L. Silencing of LncRNA HULC enhances chemotherapy induced apoptosis in human gastric cancer. J Med Biochem 2016; 35: 137-143.
5) Li Y, Lv S, Ning H, Li K, Zhou X, Xv H, Wen H. Down-regulation of CASC2 contributes to cisplatin resistance in gastric cancer by sponging miR-19a. Biomed Pharmacother 2018; 108: 1775-1782.
6) Wu X, Zheng Y, Han B, Dong X. Long noncoding RNA BLACAT1 modulates ABCB1 to promote oxaliplatin resistance of gastric cancer via sponging miR-361. Biomed Pharmacother 2018; 99: 832-838.
7) Liao HT, Huang JW, Lan T, Wang JJ, Zhu B, Yuan KF, Zeng Y. Identification of the aberrantly expressed LncRNAs in hepatocellular carcinoma: a bioinformatics analysis based on RNA-sequencing. Sci Rep 2018; 8: 5395.
8) Li Y, Zhuang W, Huang M, Li X. Long noncoding RNA DDX11-AS1 epigenetically represses LATS2 by interacting with EZH2 and DNMT1 in hepatocellular carcinoma. Biochem Biophys Res Commun 2019; 514: 1051-1057.
9) Tian JB, Cao L, Dong GL. Long noncoding RNA DDX11-AS1 induced by YY1 accelerates colorectal cancer progression through targeting miR-873/CLDN7 axis. Eur Rev Med Pharmacol Sci 2019; 23: 5714-5729.
10) Liu H, Zhang Z, Wu N, Guo H, Zhang H, Fan D, Nie Y, Liu Y. Integrative analysis of dysregulated lncRNA-associated ceRNA network reveals functional lncRNAs in gastric cancer. Genes (Basel) 2018; 9(6). pii: E303. doi: 10.3390/genes9060303.
11) Weidle UH, Birzele F, Nopora A. Pancreatic ductal adenocarcinoma: MicroRNAs affecting tumor growth and metastasis in preclinical *in vivo* models. Cancer Genomics Proteomics 2019; 16: 451-464.

12) Du Y, Shen L, Zhang W, Ding R, Li Q, Li S, Zhang H. Functional analyses of microRNA-326 in breast cancer development. Biosci Rep 2019; 39(7). pii: BSR20190787.

13) Jiang H, Liang M, Jiang Y, Zhang T, Mo K, Su S, Wang A, Zhu Y, Huang G, Zhou R. The lncRNA TDRG1 promotes cell proliferation, migration and invasion by targeting miR-326 to regulate MAPK1 expression in cervical cancer. Cancer Cell Int 2019; 19: 152.

14) Liang X, Li Z, Men Q, Li Y, Li H, Chong T. miR-326 functions as a tumor suppressor in human prostatic carcinoma by targeting Mucin1. Biomed Pharmacother 2018; 108: 574-583.

15) Ji S, Zhang B, Kong Y, Ma F, Hua Y. miR-326 inhibits gastric cancer cell growth through downregulating NOB1. Oncol Res 2017; 25: 853-861.

16) Kjersem JB, Ikdahl T, Lingjaerde OC, Guren T, Tveit KM, Kure EH. Plasma microRNAs predicting clinical outcome in metastatic colorectal cancer patients receiving first-line oxaliplatin-based treatment. Mol Oncol 2014; 8: 59-67.

17) Lima MH, Ueno M, Thirone AC, Rocha EM, Carvalho CR, Saad MJ. Regulation of IRS-1/SHP2 interaction and AKT phosphorylation in animal models of insulin resistance. Endocrine 2002; 18: 1-12.

18) Baserga R. The contradictions of the insulin-like growth factor 1 receptor. Oncogene 2000; 19: 5574-5581.

19) Yang M, Shan X, Zhou X, Qiu T, Zhu W, Ding Y, Shu Y, Liu P. miR-1271 regulates cisplatin resistance of human gastric cancer cell lines by targeting IGF1R, IRS1, mTOR, and BCL2. Anticancer Agents Med Chem 2014; 14: 884-891.

20) Fang Z, Chen W, Yuan Z, Liu X, Jiang H. LncRNA-MALAT1 contributes to the cisplatin-resistance of lung cancer by upregulating MRP1 and MDR1 via STAT3 activation. Biomed Pharmacother 2018; 101: 536-542.

21) Yao Y, Zhang T, Qi L, Zhou C, Wei J, Feng F, Liu R, Sun C. Integrated analysis of co-expression and ceRNA network identifies five lncRNAs as prognostic markers for breast cancer. J Cell Mol Med 2019; 23: 8410-8419.

22) Li Y, Li C, Li D, Yang L, Jin J, Zhang B. lncRNA KCNQ1OT1 enhances the chemoresistance of oxaliplatin in colon cancer by targeting the miR-34a/ATG4B pathway. Onco Targets Ther 2019; 12: 2649-2660.

23) Wang H, Li H, Zhang L, Yang D. Overexpression of MEG3 sensitizes colorectal cancer cells to oxaliplatin through regulation of miR-141/PDCD4 axis. Biomed Pharmacother 2018; 106: 1607-1615.

24) Li Y, Gao Y, Xu Y, Ma H, Yang M. Down-regulation of miR-326 is associated with poor prognosis and promotes growth and metastasis by targeting FSCN1 in gastric cancer. Growth Factors 2015; 33: 267-274.

25) Metz HE, Karg J, Busch SE, Kim KH, Kurland BF, Abberbock SR, Randolph-Habecker J, Knoblaugh SE, Kolls JK, Whtite MF, Houghton AM. Insulin receptor substrate-1 deficiency drives a proinflammatory phenotype in KRAS mutant lung adenocarcinoma. Proc Natl Acad Sci U S A 2016; 113: 8795-8800.

26) Wang Y, Zhang X, Zou C, Kung HF, Lin MC, Dress A, Wardle F, Jiang BH, Lai L. miR-195 inhibits tumor growth and angiogenesis through modulating IRS1 in breast cancer. Biomed Pharmacother 2016; 80: 95-101.

27) Xing AY, Wang B, Shi DB, Zhang XF, Gao C, He XQ, Liu WJ, Gao P. Deregulated expression of miR-145 in manifold human cancer cells. Exp Mol Pathol 2013; 95: 91-97.

28) Baricevic I, Roberts DL, Renehan AG. Chronic insulin exposure does not cause insulin resistance but is associated with chemo-resistance in colon cancer cells. Horm Metab Res 2014; 46: 85-93.